Research Article Vol. 3, No. 5 / 15 May 2020 / OSA Continuum 1314

OSA CONTINUUM

Dynamic control of Bessel beams through high-phase diffractive axicons

BENJAMIN K. GUTIERREZ,[1] JEFFREY A. DAVIS,[1] MARÍA M. SÁNCHEZ-LÓPEZ,[2,3] IGNACIO MORENO,[2,4,*] AND DON M. COTTRELL[1]

[1] *Department of Physics, San Diego State University, San Diego, California 92182-1233, USA*
[2] *Instituto de Bioingeniería, Universidad Miguel Hernández de Elche, 03202 Elche, Spain*
[3] *Departamento de Física Aplicada, Universidad Miguel Hernández de Elche, 03202 Elche, Spain*
[4] *Departamento de Ciencia de Materiales, Óptica y Tecnología Electrónica, Universidad Miguel Hernández de Elche, 03202 Elche, Spain*
[*] *i.moreno@umh.es*

Abstract: In this work, we present the realization of a high-phase diffractive axicon. For that purpose, we use a spatial light modulator that exhibits 10π phase modulation. We compare the results with standard diffractive axicons that exhibit 2π phase modulation. We show that high-phase modulation axicons generate Bessel beams with a shorter range and a smaller radius than standard axicons with the same period. We also find that the higher phase modulation regime provides improved diffraction efficiency since fringing effects are reduced. Therefore, dynamic control of Bessel beams is presented, controlled through the phase modulation dynamic range.

1. Introduction

Bessel beams, first introduced by Durnin [1], are beams whose electric field transversal profiles are Bessel functions that are non-diffracting with distance [2]. There are multiple ways to approximate these beams and such methods have found applications in materials processing and microfabrication [3], medical imaging [4], and optical trapping [5]. The specific techniques used to generate these non-diffracting beams include placing a narrow annular slit one focal length away from an imaging lens [6], using a conical lens or refractive axicon [7], or encoding a diffractive axicon as a hologram, typically onto a spatial light modulator (SLM) [8–10].

In certain applications it is desirable to have dynamic control of the maximum length and cross-sectional width of the Bessel beam or line focus. In refractive axicons this is achieved by changing the apex angle of the conical prism. In diffractive axicons this is achieved by changing the period of the circular grating. Past work has shown that higher order diffraction from binary patterns can produce higher-order Bessel functions with variable length and width profiles [11]. However, the energy present in these higher orders is small compared to the first order.

In this paper, we show how the maximum propagation length and the beam width of an approximate Bessel beam can be varied by application of diffractive axicons encoded onto a SLM with high-phase dynamic range. We introduce the maximum phase modulation as a new parameter to dynamically control the Bessel beam, in addition to the standard parameter, the grating period. Particularly, we examine how the line focus in the output plane is manipulated when the encoded phase depth reaches as high as 10π radians.

In our previous work, we demonstrated how such high phase modulation SLMs are very useful to overcome certain restrictions imposed by the limited spatial resolution of the device. We showed that they can produce efficient lenses with focal lengths lower than the Nyquist limit [12]. In this work, we now show how this high phase modulation regime can overcome certain limits inherent to diffractive axicons displayed onto SLMs.

#392842 https://doi.org/10.1364/OSAC.392842
Journal © 2020 Received 13 Mar 2020; revised 10 Apr 2020; accepted 10 Apr 2020; published 11 May 2020

OSA CONTINUUM

2. Diffractive axicons encoded onto SLMs with large phase modulation

The diffractive axicon is a radial grating [8] given by the phase-only function $\exp(-i2\pi r/r_0)$ with a period of r_0=$p\Delta$, where p is the number of pixels per period and Δ is the pixel pitch. In a standard diffractive axicon, the phase varies linearly from zero to 2π along each period r_0. In this work, however, we consider that the phase changes from zero to a maximum value of $M2\pi$ where M is an integer value. In general, such high phase modulation results in the effective decrease in grating period [13]. This can be expressed by the modified diffraction grating equation:

$$\theta \cong \sin\theta = M\frac{\lambda}{r_0}, \tag{1}$$

where θ is the diffraction angle, that is considered in the paraxial small angle approximation. Since most of the energy is diffracted into the $n = M^{th}$ order when M is an integer value [13], Eq. (1) considers this diffraction order only.

The maximum length of the Bessel beam generated by a diffractive axicon can be expressed as [14]

$$z_{\max} = \frac{R_{\max}}{\tan\theta} \cong \frac{R_{\max}}{\theta}, \tag{2}$$

where $R_{\max}$ is the maximum radius of the axicon. When a diffractive axicon is encoded onto a pixelated SLM, its maximum radius becomes $R_{\max}$=$N\Delta/2$, where $N\times N$ is the total number of pixels available on the SLM to encode the phase mask. Therefore, Eq. (2) becomes [8]:

$$z_{\max} = \frac{r_0}{\lambda M}\frac{N\Delta}{2} = \frac{pN\Delta^2}{2\lambda M}. \tag{3}$$

Note that as the period p decreases or as M increases, the range of the Bessel beam decreases.

Similarly, high phase modulation affects the beam width. The beam width of the zero-order Bessel function is related to the diffraction angle by [8,14]:

$$w = \frac{4.81}{k\theta} = 0.766\frac{\lambda}{\theta}. \tag{4}$$

Therefore, applying Eq. (1) the beam width of the Bessel beam is now described by

$$w = 0.766\frac{r_0}{M} = 0.766\frac{p\Delta}{M}. \tag{5}$$

This relation shows that as p decreases or as the phase depth M increases, the width of the Bessel beam decreases.

Equations (3) and (5) show that the maximum length and the width of the Bessel beam can be controlled by the ratio p/M. In standard diffractive axicons with M=1, the period p is the only parameter that can be used for controlling the Bessel beam dynamics. However, in SLMs that exhibit large phase modulation, M is another parameter useful to perform this control. This is relevant because short and narrow Bessel beams require low values of p. However, SLMs are affected by the fringing effect [15,16], a pixel crosstalk that reduces the effective phase modulation and diffraction efficiency when gratings with low period are displayed. This effect is even more relevant in devices with small pixels. Therefore, having another physical mechanism to provide the dynamic control of the Bessel beam becomes interesting. In this work we focus on using the phase depth for this purpose.

Equations (3) and (5) show that increasing the phase depth (M) of a diffractive axicon with a constant grating period causes a steeper diffraction angle which results in a diffractive axicon that can produce Bessel beams of variable length and beam width.

OSA CONTINUUM

3. Experimental set-up

Figure 1 shows the experimental setup used in this work. The light source is an Argon laser from Modu-Laser (Stellar-Pro model). We use a Semrock spectral filter to select the 458 nm output wavelength of the laser. A New Focus neutral density filter enables attenuation control over the system. The beam is then passed through a 458 nm half-wave plate (WP) to adjust the laser linear polarization along the liquid crystal director axis of the SLM. In order to clean up the beam, it is first spatially filtered and then collimated. A one-inch non-polarizing beam splitter (NPBS) directs the beam on to the SLM screen. Finally, the desired light is reflected by the SLM and passes again through the NPBS to a WinCamD CCD detector. When an axicon phase pattern is addressed to the LCoS-SLM, an approximate Bessel beam is formed on the reflected beam.

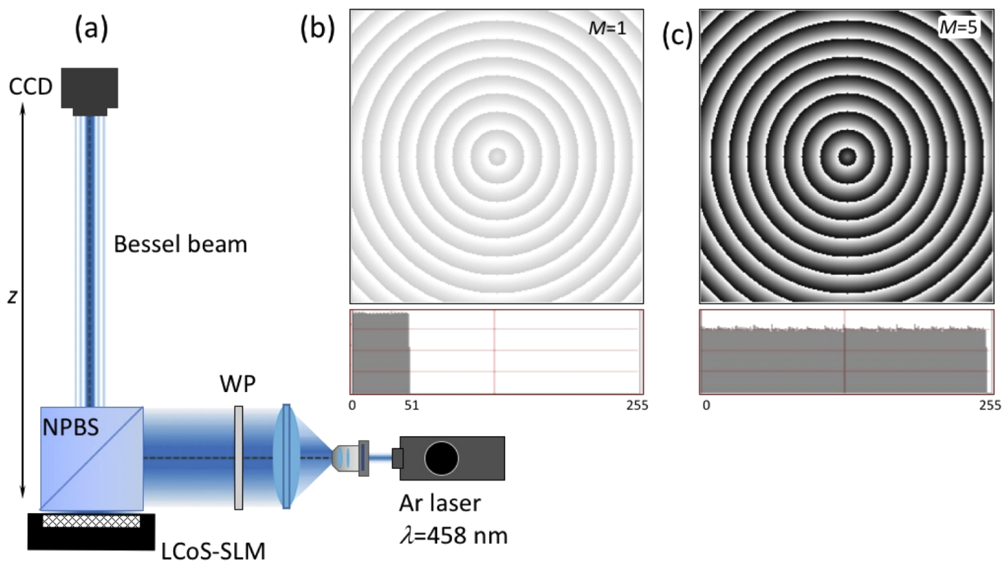

Fig. 1. (a) Diagram of the experimental setup. (b)-(c) Expanded gray-level pattern for axicons with (c) M=1 and (c) M=5. The gray level histogram is shown under each pattern.

The SLM is a reflective liquid-crystal on silicon (LCoS) device from Hamamatsu (model X10468-08) designed for use in the 1000–1500 nm wavelength range. This device consists of 792×600 pixels with a pixel spacing of Δ=20 µm. The phase patterns are formed on a 1024×1024 array and overfill the LCoS screen. This phase modulation is controlled with the addressed gray level which uses a one-byte sequence (256 levels). The device was calibrated by placing it between crossed polarizers and studying the reflection as a function of gray level [12]. The phase calibration results are equivalent to those presented in [17] for the same wavelength and the same device. Because the device is intended for use in the IR long wavelength range, it has a thick liquid-crystal layer. Therefore, by using the 458 nm wavelength, we can operate at phase depths up to 10π radians.

However, there are two problems that arise because the AR coating for the front window of the device is designed for the IR range. First, we get a strong reflection of the incident beam. In this case, this reflection will be collimated and results in a background noise added to the Bessel beam generated by the encoded axicon. Secondly, multiple internal reflections are produced in the SLM. The desired beam goes through the liquid crystal layer, reflects, and is transmitted through the window with the desired phase shift. However, part of this beam is again reflected by the window and passes again through the liquid crystal layer and has twice the phase shift. These two beams can cause interference effects. Luckily, in the case of the axicon, these multiple reflections generate additional higher-order Bessel beams, but they have much shorter range and, therefore, the main desired Bessel beam is isolated if we look far enough from the SLM. These effects could be avoided if the SLM had an AR coating designed for visible light.

Despite these effects, values of M=1, 2, 3, 4 and 5 (phase modulation of 2π, 4π, 6π, 8π and 10π, respectively) can be achieved, where the phase range in each case is controlled with gray-level values from zero to a maximum of 51, 101, 150, 199 and 252, respectively. Figures 1(b) and 1(c) show an expanded view of the phase pattern for the axicon. This phase range would be converted to a gray level pattern. To encode the standard diffractive axicon with M=1, we use gray-level values ranging only from 0 to 51 as in Fig. 1(b). As we increase the gray level range, we increase the phase modulation depth and the case M=5 is achieved when the gray-level ranges from 0 to 252 as in Fig. 1(c).

4. Experimental results

Figure 2 shows the intensity of the Bessel beam as a function of distance. Measurements were taken by placing a small aperture in front of a Newport detector in order to filter out the previously mentioned beam that is reflected from the SLM AR coating.

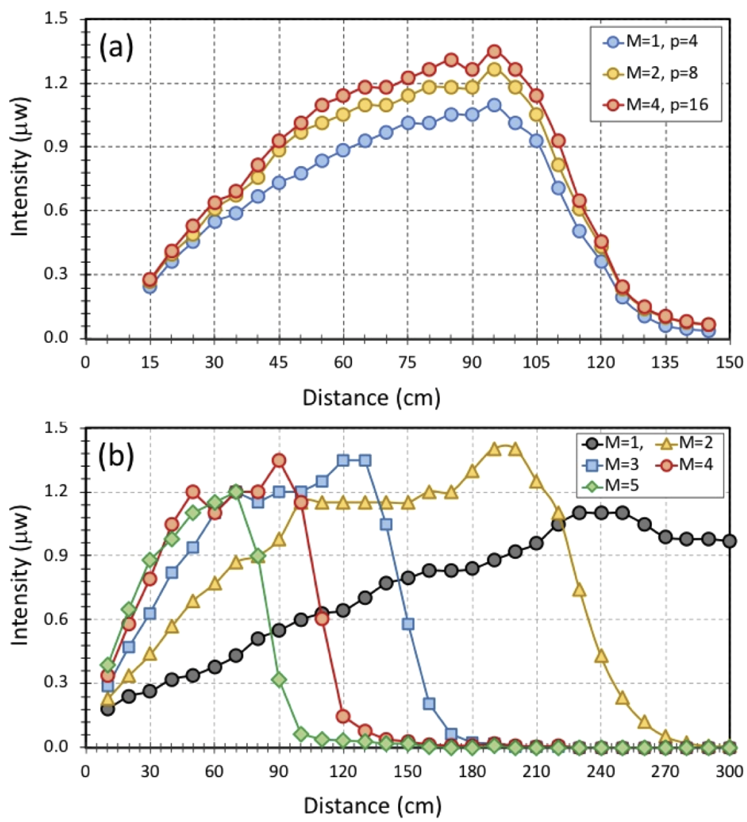

Fig. 2. Intensity versus propagation distance for Bessel beams generated by: (a) axicons with constant p/M ratio and phase depths M=1, M=2 and M=4; (b) axicons of period p=16 and phase depths M=1 through 5.

Figure 2(a) compares the results obtained using three different diffractive axicons of phase depths M=1, M=2, and M=4 with periods p=4, p=8, and p=16, respectively. In principle these cases are equivalent according to Eqs. (3) and (5) since they share the same ratio p/M. However,

OSA CONTINUUM

there is an increase of about 25% in the intensity all along the line focus in the high phase modulation version (M=4) in comparison with the standard case (M=1). This clearly shows the advantage of using grating with larger periods instead of using values as low as p=4, where diffraction efficiency diminished due to the fringing effect [15,16].

The intensity profiles follow the typical behavior of Bessel beams generated with standard axicons, where the axial intensity grows until a distance of maximum intensity after which it rapidly decays [14]. Although certain other axicon profiles could be designed to provide different axial intensity behavior [18], here we employ the standard axicon design for simplicity.

Figure 2(b) shows additional results, but now the five different phase depth values are selected with a constant period of p=16 pixels. This period ensures that there is reasonably high diffraction efficiency for all cases [13] but also gives Bessel beam ranges that can fit within the laboratory space. The figure shows how the length of the Bessel beam shortens as the phase depth is increased, decreasing by about a factor of 1/M as predicted by Eq. (3). Theoretical calculations predict the maximum length for a Bessel beam produced by a 16-pixel period axicon of phase depth M=1, 2, 3, 4 and 5 to be z_{max}=419, 210, 140, 105 and 84 cm, respectively. Although it is not clear at what point the experimental range limit should be defined (because we are affected by interference with background collimated beam reflected at the AR coating), in all cases the observed intensity decay started slightly before the theoretical predictions, as indicated in Table 1. This small reduction in the range is caused by the deformation of the SLM screen, that induces certain aberration, as described below.

Table 1. Theoretical and experimental bessel beam maximum range (z_{max}) [a].

Phase Depth (M)	Theoretical Range [cm]	Measured Range [cm][b]
1	419	–
2	210	200
3	140	130
4	105	100
5	84	70

[a]Results shown for a Bessel beam produced by a high phase dynamic axicon of period p=16.
[b]Measured range for M=1 exceed laboratory space.

Figure 3 shows the transverse beam intensity captured at various distances for different values of M. Here the period is kept constant at p=16 pixels in all these cases. Despite the interference effects with other reflected beams, as described above, these images clearly demonstrate the two main facts associated with these high-phase axicons: 1) the shorter propagation length of the Bessel beam and 2) the tighter beam radius as the value of M increases. In all cases the beam propagates for a given distance and then disappears as predicted. Cases with higher M values show, although distorted, the characteristic Bessel beam concentric rings.

Finally, we measured the width of the Bessel beam as a function of M. In these measurements, we increased the period to $p = 32$ pixels. When we used the value of 16 pixels, the resolution of the camera was limited (the camera has 4.65 µm pixels) and we could not obtain accurate enough values for the width. By doubling the period, we were able to double the beam widths so they could be resolved.

Figure 4 shows the transversal intensity profiles generated by axicons of 32-pixel period and different values of M. For these measurements, we moved the CCD detector to obtain the least amount of interference with the other beams as discussed earlier. Measurements were taken at distances of 141, 185, 108, 58, and 25 cm respectively. Theoretical calculations given by Eq. (5) predict the width of a Bessel beam produced by an axicon of phase depth M=1, 2, 3, 4 and 5 to be w=490, 245, 163, 123 and 98 µm, respectively. Measurements of the beam width confirm this prediction, showing a width reduction as M increases. These results are tabulated in Table 2.

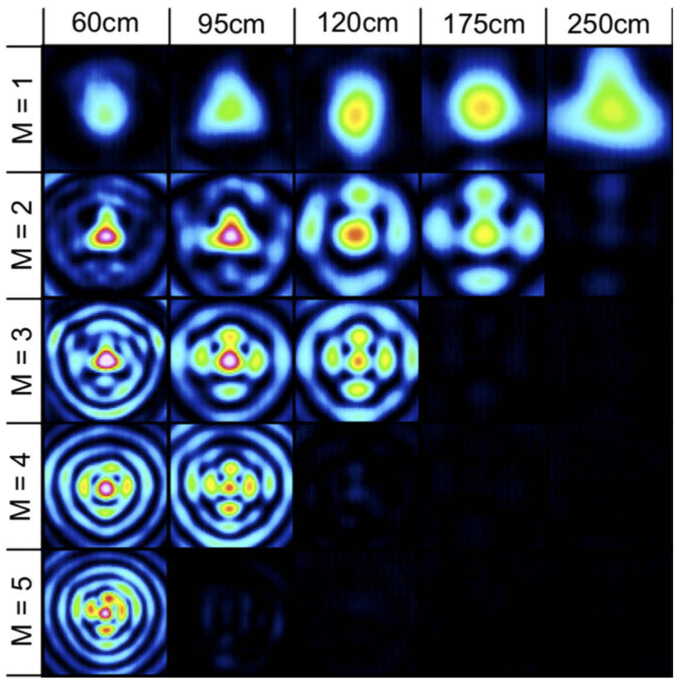

Fig. 3. Transverse images for Bessel beams generated with axicons of period p=16 and phase depths M=1 through 5 captured at various distances along the optical axis.

Table 2. Theoretical and Experimental Bessel Beam Widths[a].

Phase Depth (M)	Theoretical Width [μm]	Measured Width [μm]
1	490	365
2	245	188
3	163	121
4	123	102
5	98	79

[a]Results shown for a Bessel beam produced by a high phase dynamic axicon of period p=32.

However, we noted a disagreement of about 20% between experimental widths and theoretical predictions, where the measured widths are consistently narrower than theory. We believe this is caused by the fact that there is deformation in the SLM producing a phase wave-front distortion [19]. The manufacturer provides a correction pattern, but it is for the IR wavelengths. However, since the correction pattern has a shape close to be a quadratic phase, we could check this by adding a lens pattern to the axicon pattern. We found that the beam width increased if we used a diverging lens with a very long focal length and decreased with a converging lens. In both cases, we used focal lengths of about 25 meters. This value approximately matches correction patterns provided by the manufacturer. Additionally, we noted that the range measurements in Table 1 were less affected, by less than 10%. This smaller effect is due to the extremely long focal length of this aberration and the uncertainty of the theoretical values for the range equation.

OSA CONTINUUM

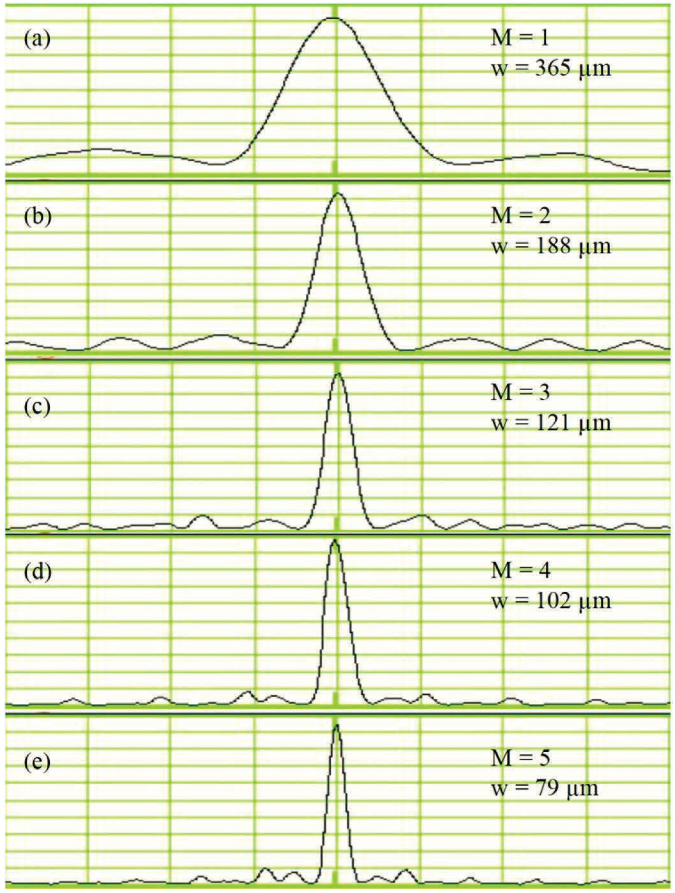

Fig. 4. Widths of Bessel beams produced by an axicon of period p=32 and phase depth (a) M=1, (b) M=2, (c) M=3, (d) M=4 and (e) M=5.

5. Conclusions

In summary, this work demonstrates the ability of high phase diffractive axicons to exhibit dynamic spatial control of the resulting Bessel beam, controlled through the phase modulation maximum dynamic range. These high phase axicons can produce Bessel beams whose radius and length are more strictly confined than previously demonstrated with standard diffractive axicons of the same period showing only 2π phase modulation. Thus, the phase modulation depth enables a new control parameter for diffractive axicons in addition to the usual method of varying its period. The greater the phase depth, the more confined the beam profile becomes and the shorter the propagation distance is.

In addition, we noted in Fig. 2(a) that the intensity of the beam increases as the value of M increases. We believe this is a result of fringing effect, which reduces diffraction efficiency when gratings with low period are encoded onto SLMs with small pixels. The use of higher values of M allows employing gratings with larger periods, therefore reducing the impact of this fringing effect.

Encoding gratings in these large phase modulation devices additionally provide an opposite chromatic dispersion in comparison to standard diffractive components [17], and therefore could be useful for use with polychromatic light. Other modulation technologies such as fluidic lenses [20] or continuous liquid-crystal lenses [21], have been used to generate refractive tunable axicons that exhibit various cycles of phase modulation. Our approach here can be considered as an intermediate situation in between pure diffractive axicons and pure refractive axicons, since the large phase modulation SLM allows changing both the period p and the modulation range M, thus providing great flexibility.

Finally, this ability to dynamically manipulate the maximum length and beam width of a Bessel beam can be useful in the different kinds of applications where a flexible and tunable Bessel beams are required. These include medical applications like laser eye surgery or optical coherence tomography, or commercial applications like laser microfabrication, optical trapping or optical alignment systems.

Funding

Conselleria d'Educació, Investigació, Cultura i Esport (PROMETEO-2017-154); Comisión Interministerial de Ciencia y Tecnología (RTI2018-097107-B-C33).

Disclosures

The authors declare no conflicts of interest.

References

1. J. Durnin, "Exact solutions for nondiffracting beams. I. The scalar theory," J. Opt. Soc. Am. A **4**(4), 651 (1987).
2. D. McGloin and K. Dholakia, "Bessel beams: diffraction in a new light," Contemp. Phys. **46**(1), 15–28 (2005).
3. F. Courvoisier, J. Zhang, M. K. Bhuyan, M. Jacquot, and J. M. Dudley, "Applications of femtosecond Bessel beams to laser ablation," Appl. Phys. A **112**(1), 29–34 (2013).
4. B. Park, H. Lee, S. Jeon, J. Ahn, H. H. Kim, and C. Kim, "Reflection-mode switchable subwavelength Bessel-beam and Gaussian-beam photoacoustic microscopy in vivo," J. Biophotonics **12**(2), e201800215 (2019).
5. J. Arlt, V. Garces-Chavez, W. Sibbett, and K. Dholakia, "Optical micromanipulation using a Bessel light beam," Opt. Commun. **197**(4-6), 239–245 (2001).
6. J. Durnin, J. J. Miceli Jr., and J. H. Eberly, "Diffraction-free beams," Phys. Rev. Lett. **58**(15), 1499–1501 (1987).
7. J. H. McLeod, "The axicon: a new type of element," J. Opt. Soc. Am. **44**(8), 592 (1954).
8. J. A. Davis, J. Guertin, and D. M. Cottrell, "Diffraction-free beams generated with programmable spatial light modulators," Appl. Opt. **32**(31), 6368 (1993).
9. Z. Jaroszewicz, V. Climent, V. Duran, J. Lancis, A. Kolodziejczyk, A. Burvall, and A. T. Friberg, "Programmable axicon for variable inclination of the focal segment," J. Mod. Opt. **51**(14), 2185–2190 (2004).
10. A. Dudley, T. Mhlanga, M. Lavery, A. McDonald, F. S. Roux, M. Padgett, and A. Forbes, "Efficient sorting of Bessel beams," Opt. Express **21**(1), 165 (2013).
11. J. A. Davis, E. Carcole, and D. M. Cottrell, "Nondiffractive interference patterns generated with programmable spatial light modulators," Appl. Opt. **35**(4), 599 (1996).
12. B. K. Gutierrez, J. A. Davis, I. Moreno, and D. M. Cottrell, "Encoding lenses with focal lengths lower than the Nyquist limit using high phase-modulation displays," Opt. Lett. **44**(13), 3398 (2019).
13. I. Moreno, B. K. Gutierrez, M. M. Sanchez-Lopez, J. A. Davis, H. P. Khanal, and D. M. Cottrell, "Diffraction efficiency of stepped gratings using high phase-modulation spatial light modulator," Opt. Laser Eng. **126**, 105910 (2020).
14. J. Turunen, A. Vasara, and A. T. Friberg, "Holographic generation of diffraction-free beams," Appl. Opt. **27**(19), 3959 (1988).
15. C. Lingel, T. Haist, and W. Osten, "Optimizing the diffraction efficiency of SLM-based holography with respect to the fringing field effect," Appl. Opt. **52**(28), 6877 (2013).
16. T. Lu, M. Pivnenko, B. Robertson, and D. Chu, "Pixel-level fringing-effect model to describe the phase profile and diffraction efficiency of a liquid crystal on silicon device," Appl. Opt. **54**(19), 5903 (2015).
17. V. Calero, P. Garcia-Martinez, J. Albero, M. M. Sanchez-Lopez, and I. Moreno, "Liquid-crystal spatial light modulator with very large phase modulation operating in high harmonic orders," Opt. Lett. **38**(22), 4663 (2013).
18. T. Cizmar and K. Dholakia, "Tunable Bessel light modes: engineering the axial propagation," Opt. Express **17**(18), 15558 (2009).
19. L. Teng, M. Pivnenko, B. Robertson, R. Zhang, and D. Chu, "A compensation method for the full phase retardance nonuniformity in phase-only liquid crystal on silicon spatial light modulators," Opt. Express **22**(21), 26392 (2014).
20. G. Milne, G. D. M. Jeffries, and D. T. Chiu, "Tunable generation of Bessel beams with a fluidic axicon," Appl. Phys. Lett. **92**(26), 261101 (2008).
21. A. K. Kirby, P. J. W. Hands, and G. D. Love, "Liquid crystal multi-mode lenses and axicons based on electronic phase shift control," Opt. Express **15**(21), 13496 (2007).